

Novel two-stage processes for optimal chemical production in microbes

Kaushik Raj^{1,*}, Naveen Venayak^{1,*}, and Radhakrishnan Mahadevan^{1,2,**}

¹Department of Chemical Engineering and Applied Chemistry, University of Toronto, Canada

²Institute of Biomaterials and Bioengineering, University of Toronto, Canada

*These authors contributed equally

**Corresponding author. Address: 200 College Street, Toronto, Ontario - M5G 2J8, Canada.

Email: krishna.mahadevan@utoronto.ca

Abstract

Microbial metabolism can be harnessed to produce a broad range of industrially important chemicals. Often, three key process variables: **T**iter, **R**ate and **Y**ield (**TRY**) are the target of metabolic engineering efforts to improve microbial hosts toward industrial production. Previous research into improving the TRY metrics have examined the efficacy of having distinct growth and production stages to achieve enhanced productivity. However, these studies assumed a switch from a maximum growth to a maximum production phenotype. Hence, phenotypes with intermediate growth and chemical production for the growth and production stages of two-stage processes are yet to be explored. The impact of reduced growth rates on substrate uptake adds to the need for intelligent choice of operating points while designing two-stage processes. In this work, we develop a computational framework that scans the phenotypic space of microbial metabolism to identify ideal growth and production phenotypic targets, to achieve optimal TRY targets. Using this framework, with *Escherichia coli* as a model organism, we compare two-stage processes that use dynamic pathway regulation, with one-stage processes that use static intervention strategies, for different bioprocess objectives. Our results indicate that two-stage processes with intermediate growth during the production stage always result in optimal TRY values even in cases where substrate uptake is limited due to reduced growth during chemical production. By analyzing the flux distributions for the production enhancing strategies, we identify key reactions and reaction subsystems that require perturbation to achieve a production phenotype for a wide range of metabolites in *E. coli*. Interestingly, flux perturbations that increase phosphoenolpyruvate and NADPH availability are enriched among these production phenotypes. Furthermore, reactions in the pentose phosphate pathway emerge as key control nodes that function together to increase the availability of precursors to most products in *E. coli*. The inherently modular nature of microbial metabolism results in common reactions and reaction subsystems that need to be regulated to modify microbes from their target of growth to the production of a diverse range of metabolites. Due to the presence of these common patterns in the flux perturbations, we propose the possibility of a universal production strain.

Keywords: dynamic pathway engineering, two-stage process, industrial bioprocess, phenotypic choices, production platforms, substrate uptake

28 1 Introduction

29 The use of microbes for the production of chemicals through metabolic engineering has garnered signifi-
30 cant interest in the past few decades. The naturally modular arrangement of metabolic networks makes
31 microbes amenable for use as chemical production platforms¹. Metabolic networks have a bow-tie archi-
32 tecture which allows a large number of metabolites to be produced from a few universal precursors². This
33 has allowed us to successfully engineer microbes to be biocatalysts for the production of a wide range of
34 commodity chemicals^{3,4}, pharmaceuticals^{5,6}, biofuels,^{7,8} and other natural and non-natural compounds⁹.
35 While some such production processes have been successful at an industrial scale^{10,11}, large strain develop-
36 ment costs and scale-up issues could deem many processes economically infeasible^{12,13}. Given the cost of
37 a target feedstock and product, the feasibility of industrial fermentation processes is typically determined
38 by three process metrics - **Titer**: concentration of product at the end of a fermentation batch (given in
39 *mmol/L* or *g/L* of product), **Rate/productivity**: the rate of product secretion (given in *mmol/L.h* or
40 *g/L.h* of product), and **Yield**: the amount of product produced per unit amount of substrate (given in
41 *mmol product/mmol substrate* or *g product/g substrate*) - collectively termed the **TRY** metrics¹⁴. Titer
42 and yield affect the operating expenditure of the process by impacting product separation and substrate
43 costs respectively, while productivity affects the capital expenditure by determining the scale of the re-
44 actor required. Microbial production processes undergo several rounds of strain, pathway and process
45 optimization to reach acceptable TRY targets^{15,16}.

46 Recent advancements in genome scale reconstructions of microbial metabolism have augmented the pro-
47 cess of strain development. Wild-type microbial strains have typically evolved to grow at maximal rates,
48 directing little carbon flux towards production of target compounds¹⁷. Metabolic engineering attempts to
49 alter the phenotype (or operating point in a production envelope) of these strains to enhance target chem-
50 ical production by throttling flux through growth associated reactions and/or tuning native metabolism to
51 balance pathway energy and cofactor requirements. Given a stoichiometric model of microbial metabolism
52 and substrate/nutrient uptake rates, the feasible range of chemical production characteristics in a micro-
53 bial strain can be visualized using its production envelope and yield envelope¹⁸, which map the maximum
54 product flux and maximum product yield respectively, at all possible growth rates of the microbe (Fig-
55 ure 1). Strain engineering strategies to improve TRY metrics can be broadly classified into static and
56 dynamic pathway engineering strategies. Static pathway engineering involves making gene deletions that
57 either couple the production of a target compound with the microorganism's growth¹⁹ or, simply redirect
58 more carbon flux through production pathways. These strategies are typically implemented as one-stage
59 (OS) production processes where the strain remains at a single operating point throughout the course
60 of the process (Figure 1a). Such processes result in higher yield by ensuring high relative pathway flux.
61 Recently, there has been an increased interest in dynamic pathway engineering, which involves temporally
62 controlling carbon flux through growth and production pathways. This can be achieved through the use of
63 biological logic or sensor and actuator systems composed of cellular components²⁰⁻²². These strategies are
64 implemented as two-stage (TS) production processes which start with cells in their growth stage and at
65 some point during the fermentation, production pathway genes are expressed to switch to the production
66 stage (Figure 1b). Such a decoupling of growth and production stages is thought to reduce batch times by
67 reaching maximal biomass concentrations faster and thereby increase productivity^{23,24}.

68 While stoichiometric models are effective for determining relative production metrics such as yield,

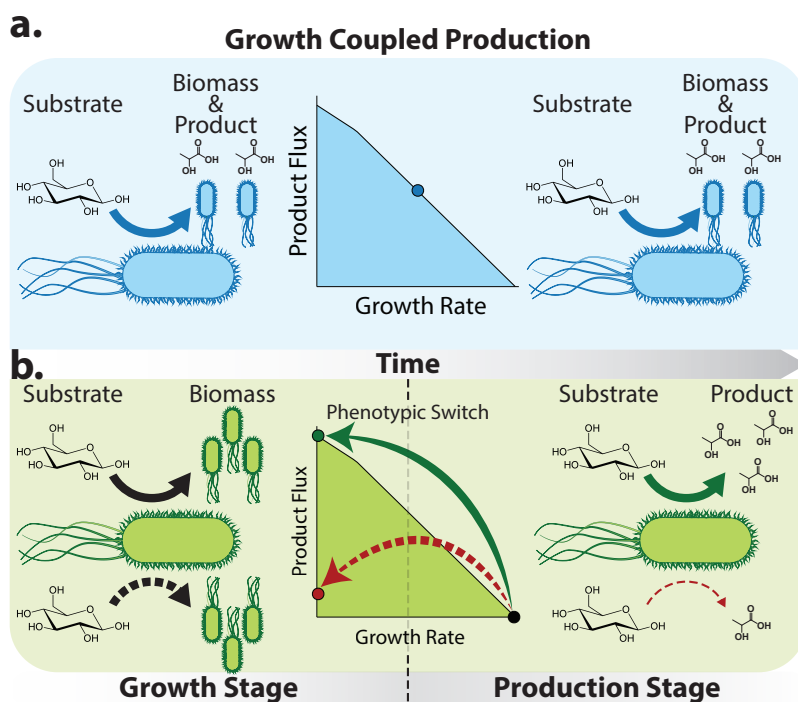


Figure 1: Static vs dynamic pathway engineering. Strain engineering strategies can be classified into **a.** Static engineering strategies where genetic perturbations that allow cells to grow and produce the target compound simultaneously (growth coupled production) are implemented. This enables the cells to produce the compound in a one-stage process. **b.** Dynamic engineering strategies where growth and production pathways are decoupled temporally. In such strategies, the process starts with a growth stage, accumulating biomass and switches over to a production stage to produce the target compound. Reduced substrate uptake during the production stage can result in lower product flux (dotted lines) than that expected assuming constant substrate uptake rates (solid lines). Hypothetical operating points for each production strategy are shown in the respective production envelopes.

69 absolute metrics such as end-titer and productivity are also governed by variations in substrate uptake
70 rates. Metabolic models with constant substrate uptake rates are routinely used for simulations to monitor
71 metabolite production rates at different phases of metabolism. The impact of reduced substrate uptake rate
72 during stationary phase metabolism²⁵ is often overlooked while designing microbial production processes.
73 Studies have shown that the rate of glucose uptake varies significantly depending on the genotype of the
74 strain and phase of metabolism²⁵⁻³¹ (Supplementary Figure S1a). A drop in substrate uptake rate during
75 the production stage of a TS process would result in reduced product flux and therefore lower productivity,
76 defeating the purpose behind designing such a process (dotted lines in Figure 1b). This effect was recently
77 shown in a theoretical study that compared the performance of TS and OS processes for D-lactic acid
78 production in *E. coli*³². This study showed that reduced substrate uptake rates can limit the advantages
79 of a TS process and in some cases, there is a very narrow range of conditions where a TS process can
80 outperform an OS process. One way to resolve this issue is to employ techniques to increase stationary
81 phase substrate uptake, such as engineering ATP futile cycles to expand the range of conditions in which TS
82 processes offer enhanced productivity. This study and many others consider only TS processes that switch
83 from wild-type growth to a non-growing production phenotype during the stationary phase of metabolism.
84 However, given the interplay between substrate uptake and growth rates, phenotypes with intermediate

85 growth and production could hold significant value. Intermediate phenotypes have been examined in the
86 past to identify operating points that result in balanced TRY values in OS processes³³.

87 In this work, we compare TS and OS production processes that make use of the entire range of fea-
88 sible production operating points rather than those with maximum growth or maximum product yield to
89 identify better production phenotypes for bioprocesses. To this end, we develop **mcPECASO** (**m**icrobial
90 **c**hemical **P**roduction **E**nhancement via **C**omplete **A**nalysis of **S**witchable **O**perating-points) - a modular
91 computational framework that can compare microbial production processes. mcPECASO uses a two-stage
92 dynamic flux balance analysis to determine the process metrics obtainable using hypothetical operating
93 points calculated within the solution space of a microbe’s metabolic model. With this information, the
94 framework can determine the best process type and optimal phenotypic choices that result in the maximum
95 value of a predetermined objective. We use mcPECASO to discover enhanced TS processes that result in
96 high TRY values while considering the substrate uptake effects of reduced growth. We also identify flux
97 perturbations that occur consistently in production strategies for all natural products, giving rise to the
98 possibility of a universal chassis for metabolic engineering.

99 2 Materials & Methods

100 The methods used in the mcPECASO formulation and the analysis of production stage fluxes are outlined
101 below.

102 2.1 mcPECASO formulation

103 The mcPECASO workflow formulated in this study is briefly summarized in Figure 2. The overall goal in
104 mcPECASO was to identify optimal phenotypic combinations for TS chemical production processes and
105 compare TS processes with OS processes towards a user defined bioprocess objective for a broad range of
106 host strains and target compounds. Therefore, we formulated mcPECASO as a modular framework where
107 the choice of host organism, target compound and fermentation parameters can be readily modified to suit
108 the user’s requirements. The individual steps involved in this formulation are described below.

109 2.1.1 Establishing substrate uptake characteristics

110 The first step towards analyzing the performance of chemical production strategies using a metabolic model
111 is establishing a relationship between the growth rate and the substrate uptake rate in the organism being
112 studied. There are several studies that have attempted to elucidate the relationship between substrate
113 uptake and growth rates in *E. coli* - the host of our choice. Many of these have examined this relationship
114 using a chemostat under glucose limiting conditions³⁴⁻³⁷. Under these conditions, the rate of glucose uptake
115 is limited by the dilution rate prevailing in the reactor and not by the effects of genetic perturbations in
116 the cells. Therefore, for our analysis we only considered studies with batch fermentations under glucose
117 excess conditions to identify the relationship between growth and substrate uptake²⁵⁻³¹ (Data attached as
118 supplementary file). Furthermore, we restricted our analysis to the MG1655 strain of *E. coli* due to its
119 ubiquitous use in research and industrial biotechnology (Supplementary Figure S1b).

120 Preliminary analysis of growth dependent substrate uptake rates in *E. coli* MG1655 did not reveal a
121 one-to-one relationship. This is possibly due to the fact that the data-points collected (Supplementary

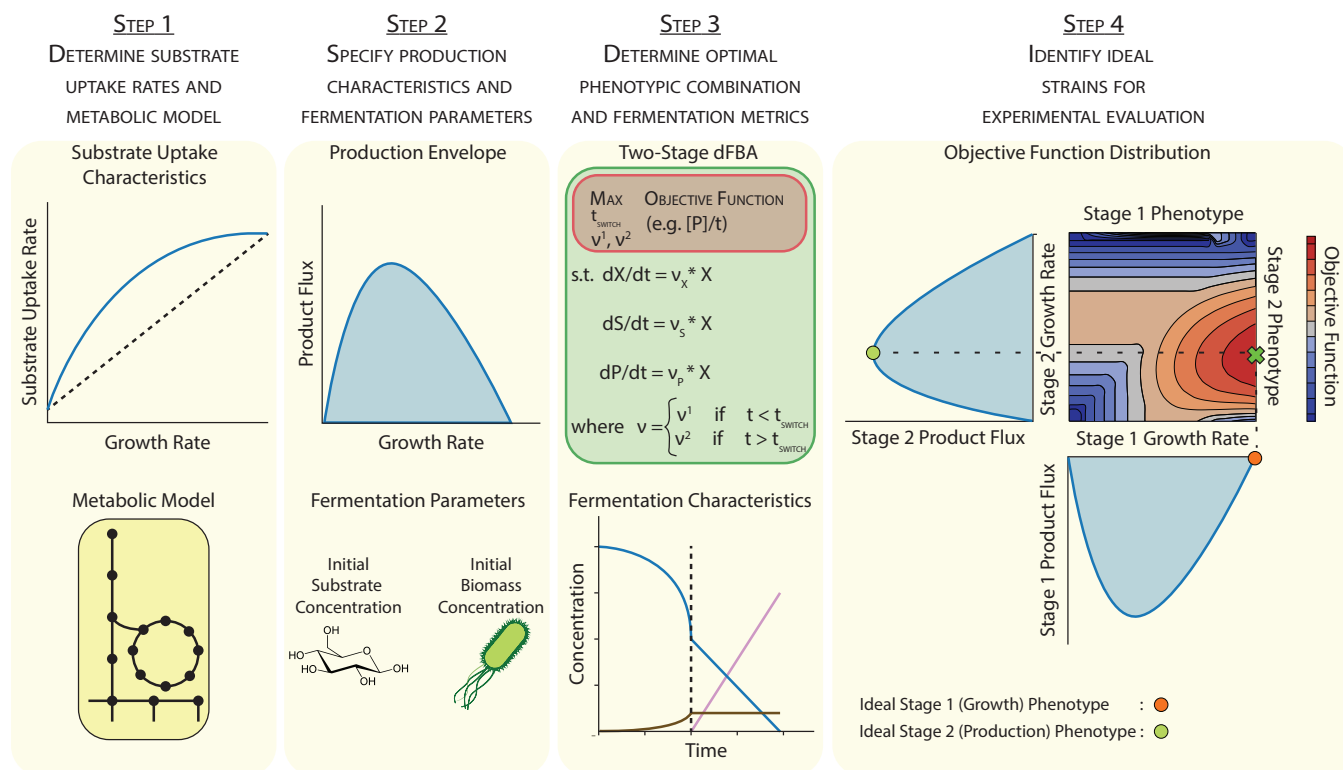


Figure 2: mcPECASO workflow. **Step 1** - A metabolic reconstruction of the microorganism and an approximation of the substrate uptake characteristics at different growth rates are given as inputs to the formulation. Currently, mcPECASO accepts all COBRA compatible metabolic models and any mathematical function to model substrate uptake variations. **Step 2** - A realistic production envelope is generated for the product of interest. This entails maximizing the product flux at all possible growth rates of the organism while considering reduced substrate uptake limitation at low growth rates. Fermentation start parameters such as initial biomass and substrate concentrations are given as inputs. **Step 3** - A two-stage dynamic flux balance analysis that maximizes a user-defined objective function (any combination of the process metrics - productivity, yield, and titer) is conducted to determine the process metrics, and optimal combination of phenotypes. **Step 4** - A distribution of process metrics for all two-stage processes is plotted and strains for experimental evaluation are chosen. The optimal phenotype for each stage has been projected onto the respective production envelope.

122 Figure S1b) belong to strains with different gene deletions and each deletion potentially affects substrate
 123 uptake and growth rates through a different mechanism. Glucose uptake regulation in *E. coli* is quite
 124 complex and controlled by global transcriptional regulators and more directly by intracellular metabolites
 125 through allosteric regulation³⁸. Direct allosteric regulation of glucose uptake has been shown to result
 126 from a build-up of intracellular metabolites involved in the citric acid cycle such as α -ketoglutarate, which
 127 competitively inhibits one of the enzymes involved in the phosphotransferase system³⁹⁻⁴¹. With the as-
 128 sumption that the levels of intracellular metabolites increase transiently upon a switch to lower growth
 129 rates due to carbon flux being partitioned towards production pathways, and that the extent of this in-
 130 crease depends on the extent of growth rate reduction, we propose that glucose uptake rates likely obey a
 131 saturation type model where glucose uptake rate increases with growth rates and saturates at its maximum
 132 value at wild-type growth. Therefore, we chose to use a logistic curve - the most commonly used saturation
 133 type model as an approximation of substrate uptake variation with growth (shown in Supplementary Text

134 1.1). The parameter values for this curve were chosen such that the model would match experimentally
135 observed substrate uptake rates at wild-type growth and stationary phase growth, while resulting in the
136 least possible substrate uptake rates at all intermediate growth rates, to represent a worst case scenario
137 for substrate uptake inhibition. Higher values of substrate uptake at intermediate growth rates will not
138 affect the conclusions of this study, as will be seen later.

139 **2.1.2 Determining a realistic production envelope**

140 The next step is to determine the range of feasible product secretion rates for the strain over its entire growth
141 range. In this study, we refer to a metabolic mode of an organism, represented by a unique combination
142 of the possible growth and product secretion rates within the solution space of its metabolic model, as an
143 operating point or ‘phenotype’. At intermediate growth rates, between the minimum and maximum values
144 for the organism, determined from the metabolic model, we derive the corresponding substrate uptake rates
145 using the relationship established in the previous step. Then, at each value of growth rate, we calculate
146 the feasible range of product secretion rate or the production envelope, by constraining the growth and
147 substrate uptake reactions to the required values and maximizing the secretion rate of the metabolite of
148 interest. This is in contrast to traditional production envelopes where substrate uptake rates are assumed
149 to be constant. Hence, while traditional production envelopes result in maximum product secretion at zero
150 growth, the substrate uptake limited production envelope results in maximum product secretion at some
151 intermediate value of growth rate. We believe that this novel mapping of product secretion to growth rates
152 is a more realistic simulation of actual production rates that can be expected in mutant strains.

153 **2.1.3 Two-stage dynamic flux balance analysis**

154 Dynamic flux balance analysis (dFBA)⁴² can be used to obtain process metrics for a fermentation process
155 by simulating substrate, biomass and product concentrations over the course of a fermentation batch,
156 provided that initial concentrations of these species are known. This is done by using ordinary differential
157 equations to simulate changes in the concentration of relevant species using their fluxes obtained from a
158 metabolic model. Here, we modify the dFBA formulation to allow for a phenotypic switch between the
159 two stages of a TS fermentation process by using distinct biomass, substrate and product fluxes in the
160 two stages as seen in Eq. 1d. In this equation, $[X]$, $[S]$, and $[P]$ represent the biomass, substrate, and
161 product concentrations respectively and $\nu_{n,X}$, $\nu_{n,S}$, and $\nu_{n,P}$ are their corresponding production fluxes in
162 the metabolic model for each stage. The biomass production flux ($\nu_{n,X}$) is set by the outer optimization
163 problem (Eq. 1a), which is described in the following section. Substrate flux ($\nu_{n,S}$) corresponding to this
164 value of $\nu_{n,X}$ is calculated using the relationship established previously. The maximum possible product
165 flux ($\nu_{n,P}$) given these constraints is obtained in an inner optimization problem by performing flux balance
166 analysis on a metabolic model by setting the product flux to be the objective and constraining the biomass
167 and substrate fluxes to required values (Eq. 1e).

168 **2.1.4 Optimizing bioprocess objective**

169 The goal of the optimization framework is to maximize either one or a weighted combination of the
170 fermentation metrics - productivity, yield and titer (Eq. 1a), which can be readily calculated from the

171 substrate and product concentrations at the end fo the fermentation batch obtained from the dynamic flux
 172 balance analysis formulation shown in Eq. 1d. This is achieved by varying the phenotypes (represented by
 173 the fluxes - ν_1 and ν_2) for the two stages, such that these phenotypes lie on the production envelope. More
 174 specifically, the biomass fluxes for each stage - $\nu_{1,X}$ and $\nu_{2,X}$ are varied in the outer optimization problem
 175 and the corresponding substrate and product fluxes are calculated as described previously. An additional
 176 design variable that affects the outcome of the fermentation batch is the time of switching between the
 177 two stages (t_{switch}), which can vary between zero and a user-defined maximum value. In addition to the
 178 constraints on the design variables (Eq. 1b), we added optional constraints on the fermentation metrics
 179 which can be used to specify a minimum required productivity/yield/titer for the optimization problem
 180 (Eq. 1c). The reasons for choosing these objectives will be elaborated in the Results & Discussion section.

$$\underset{\nu_{1,X}, \nu_{2,X}, t_{switch}}{\text{maximize}} \quad f(\text{prod.}, \text{yield}, \text{titer}) \quad (\text{Eq. 1a})$$

subject to

$$0 \leq \nu_{1,X}, \nu_{2,X} \leq \nu_{wt,X} \quad (\text{Eq. 1b})$$

$$0 \leq t_{switch} \leq t_{max}$$

$$\text{prod.} \geq \text{prod.}_{min} \quad (\text{Eq. 1c})$$

$$\text{yield} \geq \text{yield}_{min}$$

$$\text{titer} \geq \text{titer}_{min}$$

$$\frac{d[X]}{dt} = \nu_{n,X} * [X] \quad (\text{Eq. 1d})$$

$$\frac{d[S]}{dt} = \nu_{n,S} * [X]$$

$$\frac{d[P]}{dt} = \nu_{n,P} * [X]$$

$$\underset{\nu_n}{\text{maximize}} \quad c^T \nu_n \quad (\text{Eq. 1e})$$

$$\text{subject to} \quad S \cdot \nu_n = 0$$

$$\nu_{lb} \leq \nu_n \leq \nu_{ub}$$

where

$$n = \begin{cases} 1 & \text{if } t \leq t_{switch} \\ 2 & \text{if } t > t_{switch} \end{cases}$$

181 2.1.5 Packaging and availability

182 The mcPECASO framework is written as a python package that accepts COBRApy⁴³ compatible metabolic
 183 models. The modular nature of this package allows users to select a metabolic model, fermentation start

184 parameters and, substrate uptake characteristics with ease. In order to reduce run times, we allowed for the
185 optimization and dFBA calculations shown in Eq. 1 to be run parallelly on multi-core and multi-processor
186 systems. The optimization problem was implemented using the COBYLA method in the optimization
187 package of SciPy library in Python. The mcPECASO framework can be installed and run on any system
188 with a working Python 3 distribution. The framework, along with installation instructions are available
189 on GitHub⁴⁴.

190 2.2 Implementation

191 All analyses were conducted using the COBRAPy⁴³ and Cameo⁴⁵ packages on a Python 3.7 distribution.
192 *E. coli*'s genome scale metabolic reconstruction - iJO1366⁴⁶ was used to perform all simulations to compare
193 the two fermentation strategies. Unless otherwise specified, fermentation batches were started with 500
194 mM (≈ 90 g/L) of D-glucose as the substrate and 0.05 g/L of biomass. These values are in the range
195 of required substrate and biomass concentrations to achieve acceptable TRY targets¹⁵. Three different
196 bioprocess objectives were used to compare TS processes to OS processes in *E. coli*:

- 197 • *Objective I*: maximize productivity
- 198 • *Objective II*: maximize productivity with yield above a certain threshold (75% of the maximum yield
199 unless otherwise specified)
- 200 • *Objective III*: maximize yield with productivity above 2 g/L.h

201 The reasons for choosing these objectives will be elaborated in the Results & Discussion section. Wild-
202 type flux distributions were obtained through parsimonious flux balance analysis (pFBA)⁴⁷. In order to
203 minimize differences among the production stage flux distributions for all the products analyzed, we used
204 the inherent redundant nature of metabolic networks to limit the number of different reactions involved
205 in these flux distributions. This was done through several rounds of flux variability analysis (FVA)⁴⁸
206 where reactions that can be constrained to zero for all products were successively removed. In the end,
207 we obtained flux distributions for each product that only involved reactions that are either absolutely
208 necessary for the production of that compound or are used in all or many of the other products analyzed.
209 FVA and pFBA were run on the metabolic model using the IBM ILOG CPLEX (v12.9) solver and data
210 visualization was performed using the plotly package. The source code used to perform the various analyses
211 and generate figures used in this article are available on a GitHub repository⁴⁹.

212 3 Results & Discussion

213 3.1 Case Study: Production of D-Lactic Acid in *E. coli*

214 We applied the newly formulated mcPECASO framework to predict strategies that maximize the produc-
215 tivity (*Objective I* described in the Materials & Methods section) of D-lactic acid production in *Escherichia*
216 *coli*, starting with 500 mM of glucose as substrate and 0.05 g/L biomass. First, we examined the process
217 under constant substrate uptake conditions i.e. assuming that the substrate uptake is unaffected by growth
218 and other metabolic perturbations (Figure 3a). In these conditions, since the product flux and yield are
219 highest when there is no growth, the best TS process for productivity is the traditional TS process, where

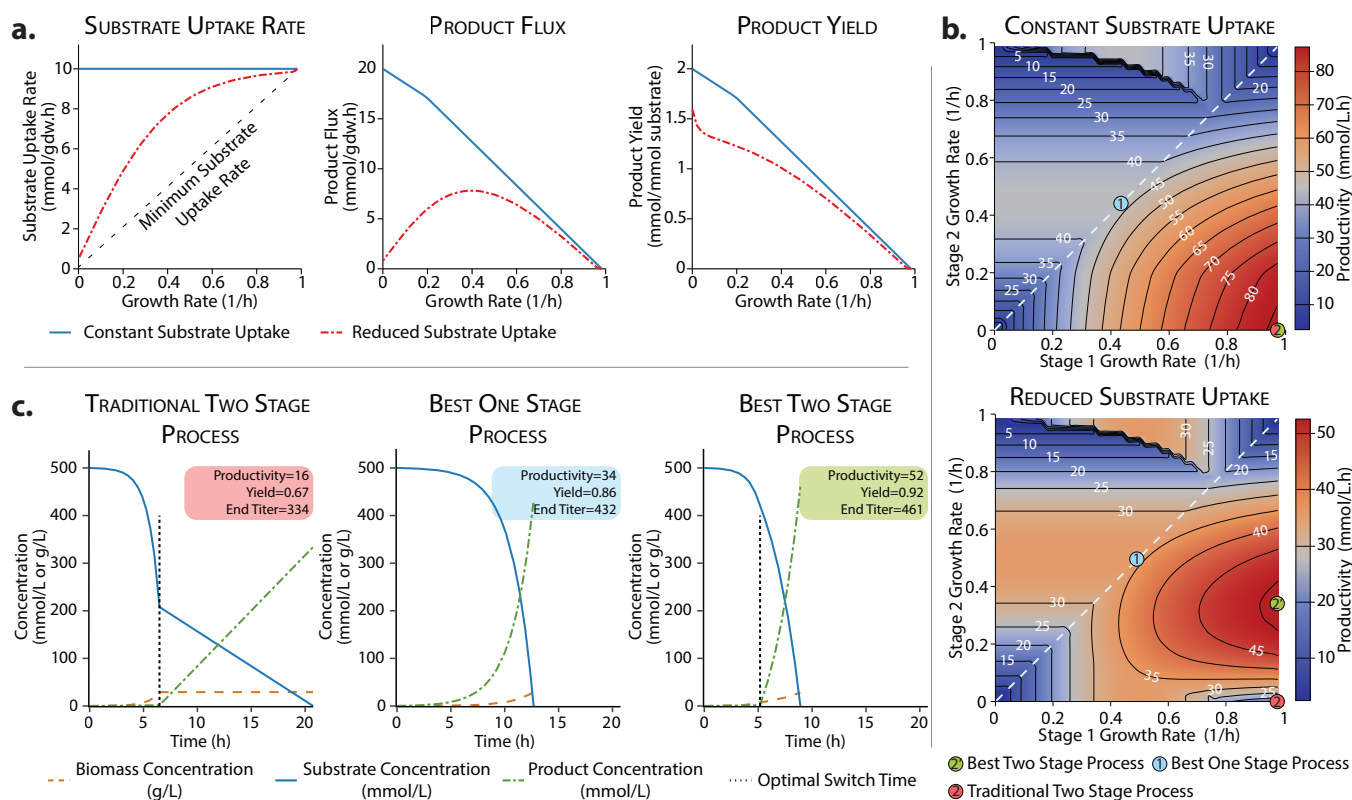


Figure 3: mcPECASO implemented for D-lactic acid production in *E. coli*. *Objective 1* - maximizing productivity **a.** substrate uptake rates, product flux and product yields obtained using the iJO1366 reconstruction of *E. coli* assuming constant and reduced substrate uptake rates. In the panel for substrate uptake rate, the minimum required substrate uptake rate at each value of growth rate (shown using a black dashed line) was obtained by performing flux balance analysis on the metabolic model by setting substrate uptake as the objective. **b.** Productivity distribution for TS and OS processes in *E. coli* assuming constant and reduced substrate uptake rates. Isoclines on the distributions show phenotypes with the same productivity levels. **c.** Fermentation profile for various production strategies assuming reduced substrate uptake rates.

220 the strain is allowed to switch from a maximum growth (wild-type) to a zero-growth phenotype (Figure 3b).
 221 As expected, the traditional TS process has a much higher productivity than the best OS process.

222 However, an impediment in growth rate either due to reaching stationary phase or rewiring of metabolism
 223 has been shown to alter substrate uptake rates^{25–31}. If these effects are considered, the product flux in
 224 a non-growing strain is heavily impacted (shown as red dashed lines in Figure 3a). This makes a non-
 225 growing phenotype during the second stage of a TS process ineffective. We can observe this in Figures 3b,c
 226 where the traditional TS process has very low productivity - among the lowest of any possible process. As
 227 observed in a previous study³², many OS processes (represented on the dashed lines in Figure 3b where
 228 the growth and production phenotypes are the same) have higher productivity than the traditional TS
 229 process. However, a fair evaluation of two-stage strategies should include the entire available phenotypic
 230 space. Even under reduced substrate uptake conditions, there are several TS processes that have higher
 231 productivity than the best performing OS process. These processes can be achieved by allowing the strain
 232 to grow at a reduced rate during the production stage, rather than completely eliminating growth. The
 233 switch time optimization formulation results in earlier switching between the phenotypes when the strain is

234 allowed to grow during the production stage (Figure 3c). The TS process with the highest productivity re-
235 quires the strain to be able to dynamically switch from wild-type growth to a phenotype with intermediate
236 growth and production (growth coupled production). A sensitivity analysis performed on the bioprocess
237 objective's response to varying the initial substrate and biomass concentration showed that TS processes
238 outperformed OS processes over a broad range of fermentation start conditions (Supplementary Figures
239 S4 and S5).

240 However, a process with the highest productivity may not always be the economically optimal choice due
241 to variations in substrate and product prices. *Objective I* aims to maximize productivity with no constraints
242 on the yield resulting from the process. Hence, to analyze TS and OS processes in a more realistic manner,
243 we examined each process type with two additional objectives - *Objective II* which maximizes productivity
244 with an added requirement that the yield must be at least 75% of the maximum value and *Objective III*
245 which maximizes yield with a minimum productivity of 2 g/L.h. These values have been previously cited
246 to be the minimum acceptable values for a bioprocess that targets commodity chemicals to be economically
247 viable¹⁵. We find that the best TS process results in higher productivity than all OS alternatives in the
248 case of *Objective II* as well (Supplementary Figures S2a and S3a). We also examined the effect of varying
249 the minimum required yield on the productivity achieved by the various process types and found that
250 TS processes result in significantly higher productivity over the entire range of possible yield constraints
251 (Supplementary Figure S6a). For *Objective III*, best performing OS process seems to result in the highest
252 yield (Supplementary Figures S2b and S3b). However, at higher requirements of productivity, the yield
253 from the OS process becomes lower than the TS process and above a certain threshold, the OS process
254 becomes infeasible since it is not possible to satisfy the productivity constraint. This shows that TS
255 processes outperform OS processes for D-lactate production in *E. coli* over a broad range of requirements
256 and fermentation start conditions if a switch from wild-type growth to an intermediate growth coupled
257 production phenotype is made.

258 3.2 TS processes are optimal for all natural metabolites in *E. coli*

259 Having established that TS processes outperform OS alternatives for lactic acid production using econom-
260 ically relevant objectives, we wished to examine if they could dominate OS processes for other natively
261 produced metabolites in *E. coli* for all three objectives. We anticipated that the different production flux
262 profiles for each product would result in variations in the process metrics. Moreover, the constraints in
263 two of the bioprocess objectives could result in different processes being more suitable for each product.
264 Hence, we used mcPECASO with the fermentation start parameters previously described, to predict pro-
265 cess optimality for 70 native exchange metabolites (metabolites that appear in exchange reactions) in the
266 iJO1366 reconstruction of *E. coli*'s metabolism. For *Objective I* and *Objective II* where the goal is to
267 maximize productivity, the best TS processes have the highest productivity for all products analyzed, with
268 the OS process and traditional TS process trailing behind (Figure 4a and Supplementary Figure S7a). In
269 general, products with more carbon atoms have lower molar productivity. However, two products, namely
270 5-methylthioribose and spermidine have unusually low productivities, which will be examined in later sec-
271 tions. The traditional TS processes have very stunted productivities for all the exchange metabolites when
272 substrate uptake rates is reduced, consistent with the previous study for D-lactic acid³².

273 Surprisingly, when feasible, TS processes result in higher yields than OS processes when the objective is

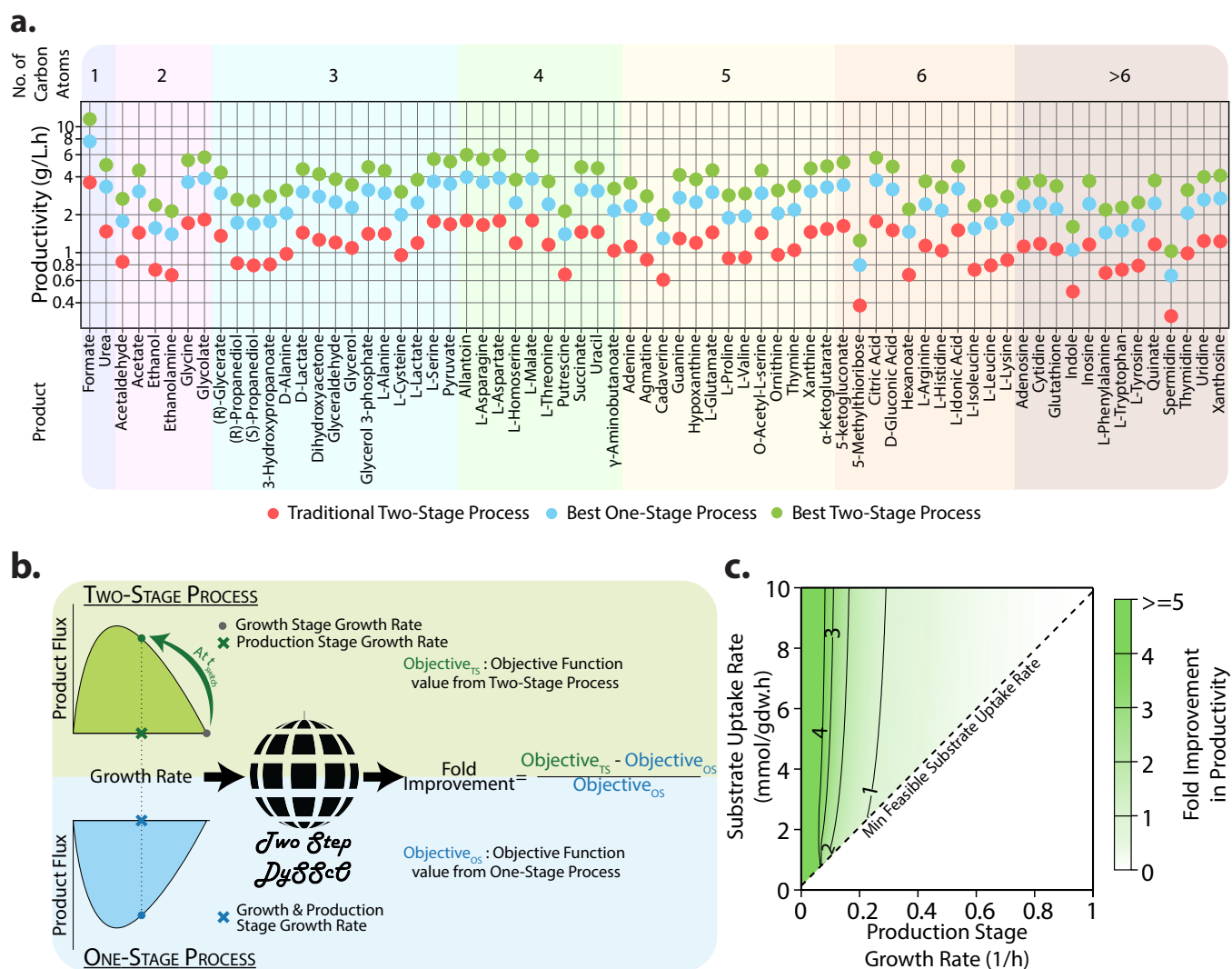


Figure 4: Comparison of TS processes for chemical production using *E. coli*. **a.** Productivity for exchange metabolite production in *E. coli*. mcPECASO was used to simulate the production of all exchange metabolites for *Objective I* - maximizing productivity in the iJO1366 reconstruction of *E. coli*, ordered by the number of carbon atoms in the product. The optimized two stage process always results in the highest productivity. **b.** Workflow to compare TS and OS processes with different substrate uptake characteristics. Production stage phenotypes for TS and OS processes are compared by computing the fold improvement in the objective function resulting from either process type. **c.** Fold improvement in productivity when using a TS process with *Objective I* - maximizing productivity for native exchange metabolites in *E. coli*. TS processes result in higher productivity at all points in the figure, indicating the superiority of such processes regardless of the substrate uptake rate prevailing during the production stage.

274 to maximize process yield with a minimum required productivity (*Objective III*) as seen in Supplementary
 275 Figure S7b. This is due to OS processes with higher yields being unable to satisfy the productivity
 276 constraint specified by *Objective III*. For the lone case of D-lactic acid, it appears that an OS process with
 277 the same yield as a TS process is able to satisfy the productivity requirement. All three process types
 278 are infeasible for three products - Spermidine, Indole, and 5-Methylthioribose. For all other products
 279 where productivity and yield requirements are feasible, TS processes dominate. OS processes even become
 280 infeasible, being unable to satisfy the productivity constraint for many products. Hence, TS processes are

281 of value even when yield maximization is the objective in an industrial setting.

282 Upon examining the best TS processes predicted by mcPECASO, we found that all of them had the
283 same phenotype during the growth stage - wild-type growth. These processes varied in phenotype only
284 during the production stage, where an intermediate growth phenotype resulted in the highest productivity.
285 Similarly, OS processes with the highest productivity are those with an intermediate growth rate and have
286 one growth-coupled production stage. Hence, it is possible to compare the two process types at every
287 operating point in the production envelope during the production stage for all possible substrate uptake
288 rates, allowing us to come to more generalizable conclusions. As stated before, the logistic curve used to
289 model substrate uptake variation is just an approximation that seeks to closely model a worst-case scenario
290 for substrate uptake rates. This analysis where we allow substrate uptake to take any value above the
291 minimum feasible rate would help in establishing the superiority of one process type over another.

292 To compare the process types for the three different objectives, we calculated the fold improvement in
293 the objective value offered by the TS process when compared to the OS process at each feasible operating
294 point (Figure 4b). For *Objective I* and *Objective II*, we found that the fold improvement in productivity
295 remained the same for all 70 products. TS processes have higher productivity at all feasible substrate
296 uptake rates for *Objective I* (Figure 4c). In the case of *Objective II*, an increase in the yield constraint
297 reduces the range of substrate uptake rates over which either process is feasible (shown by the red region
298 in Supplementary Figure S8). However, TS processes still result in higher productivity over the entire
299 feasible region of substrate uptake rates.

300 However, for *Objective III*, each product resulted in a different distribution of the fold improvement
301 in process yield. This is because the constraint on productivity is given in mass units and not molar
302 units. Regardless, we analyzed each product individually and have presented them in Supplementary
303 Figure S9. Apart from a few exceptions, OS processes are not feasible for most products over a large
304 range of substrate uptake rates. They are feasible only when the production stage growth rates and the
305 corresponding substrate uptake rates are high. At the operating points where feasible, they result in higher
306 yields. However, TS processes are optimal over a larger range of substrate uptake rates for most products
307 and are able to achieve the same yields as OS processes at lower growth rates. Moreover, for every product,
308 the highest yield obtainable using TS processes is more than the highest yield possible using OS processes,
309 as indicated by contour lines in each plot of Supplementary Figure S9. Hence, TS processes are optimal
310 for yield and productivity maximization, irrespective of the substrate uptake characteristics.

311 **3.3 Similarities in production stage fluxes suggest the possibility of a universal pro-** 312 **duction phenotype**

313 While it is clear that the enhanced TS processes obtained here are optimal for maximizing yield and
314 productivity, it would be useful to determine how such processes can be physically realized. Hence, we
315 examined the flux perturbations required to achieve the various production strategies for each of the ex-
316 change metabolites analyzed in the previous section using flux variability analysis, as described previously.
317 The best TS processes predicted by mcPECASO use wild-type growth as the phenotype in the first stage.
318 Therefore, using the wild-type flux distribution as a reference, we examined the number of reactions that
319 would need to be perturbed for each product in the three objectives (Supplementary Figures S10, S11, and
320 S12), and classified each perturbed reaction/flux them based on whether they are:

- 321 • Switched On - growth stage flux is zero and production stage flux is non-zero.
- 322 • Switched Off - growth stage flux is non-zero, production stage flux is zero.
- 323 • Significantly Upregulated - production stage flux is at least 10% more than the growth stage flux
- 324 • Significantly Downregulated - production stage flux is decreased more than biomass flux.

325 Fewer than 10 reactions need to be switched on or completely switched off for most products in all three
326 objectives to achieve the production stage. Products with fewer carbon atoms require more reactions to
327 be turned on/off and consequently, a bigger flux change compared to larger products. This suggests that
328 most of the reactions required to produce larger products optimally are expressed during wild-type growth.
329 Very few reactions need to be completely switched off for most products, implying that reactions involved
330 in biomass synthesis are required in some capacity during the production stage as well. Interestingly, the
331 compounds that were determined to have an unusually low yield in the previous section - 5-methylthioribose
332 and spermidine have among the largest number of significantly upregulated reactions of all products. The
333 yield of these products is likely low due to the upregulation of pathways that result in yield losses during
334 production and the absence of alternative pathways that conserve yield.

335 To further understand the production-stage phenotypes, we examined the magnitude of flux changes
336 from the wild-type flux distribution for every product and arranged the reactions based on the subsystem in
337 which they occur for each objective (Figure 5 and Supplementary Figure S13). Most perturbations for the
338 best TS process are downregulations, with a majority of these reactions having the same level of reduction
339 in flux as the reduction growth rate (about 60%). Hence most of the flux changes observed are effected by
340 a decrease in growth/biomass synthesis rate. This is also evident from the fact that all reactions involved
341 in membrane lipid metabolism and cell envelope biosynthesis are consistently downregulated for most
342 products. Similarly, glycolysis and citric acid cycle (TCA cycle) pathway reactions are downregulated for
343 most products. However, many reactions involved in glycolysis have a much smaller change, indicating that
344 carbon flow remains consistent through these reactions and flux is partitioned towards production pathways
345 further downstream. Interestingly, reactions in the pentose phosphate pathway are equally divided between
346 being upregulated or downregulated together for different products. Hence, this subsystem appears to act
347 as a key node that controls precursor and cofactor availability to manufacture metabolites optimally within
348 the cell. These results suggest that it is possible to engineer an *E. coli* strain with a universal production
349 phenotype that maximizes productivity/yield. In such a strain, flux perturbations that appear for all the
350 products of interest can be dynamically implemented by throttling flux through key reactions contributing
351 to biomass synthesis. Then, depending on the class of product of interest - amino acid, nucleotide, central
352 carbon metabolite, etc, those reactions/pathways that require upregulation can be set up in a modular
353 manner and dynamically expressed if required.

354 **3.4 Perturbations increasing phosphoenolpyruvate and NADPH availability are en-** 355 **riched**

356 In order to identify key control reactions, we analyzed which reactions are enriched in production strategies
357 for the exchange metabolites previously analyzed. We did this by looking at the number of products for
358 which each reaction appeared as a perturbation and classified them based on the type of perturbation -

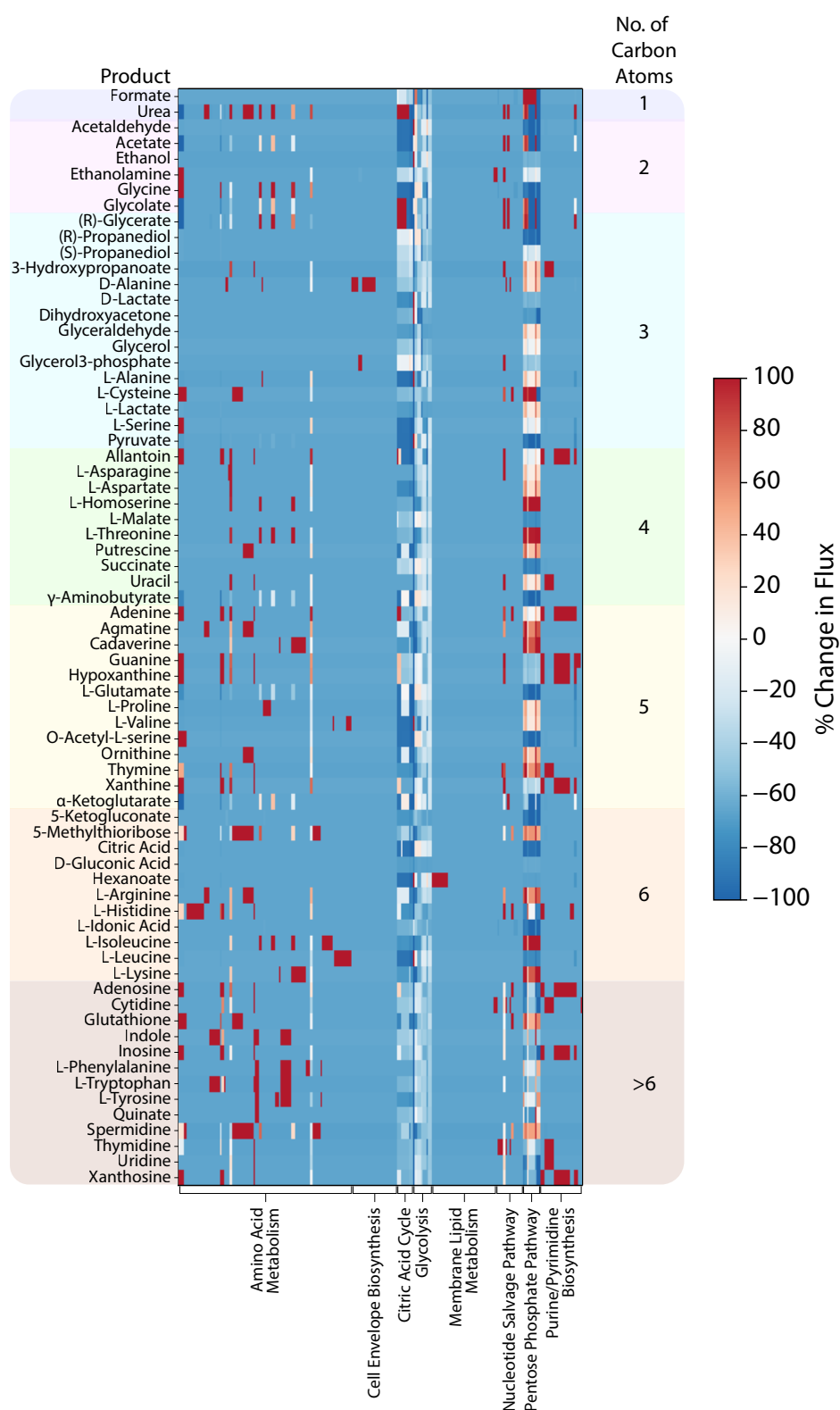


Figure 5: Flux perturbations required for TS processes. Percent change in flux through all reactions compared to wild-type flux distribution required to achieve the TS processes for native exchange metabolites in *E. coli* for *Objective I* - maximizing productivity. Due to the large number of reactions involved, only the reaction subsystems are shown. A large number of reactions show a 60% reduction in flux for all products, which is caused by an identical decrease in growth rate. Flux changes that are not effected by growth rate reduction are mostly localized to specific reaction subsystems.

359 on, off, upregulated or downregulated for each objective (Figure 6 and Supplementary Figure S14). Only
 360 non-transport reactions involved directly in metabolism were retained for the final analysis. The full names
 361 of reactions and their corresponding reaction formulae are available in Supplementary Table S1.

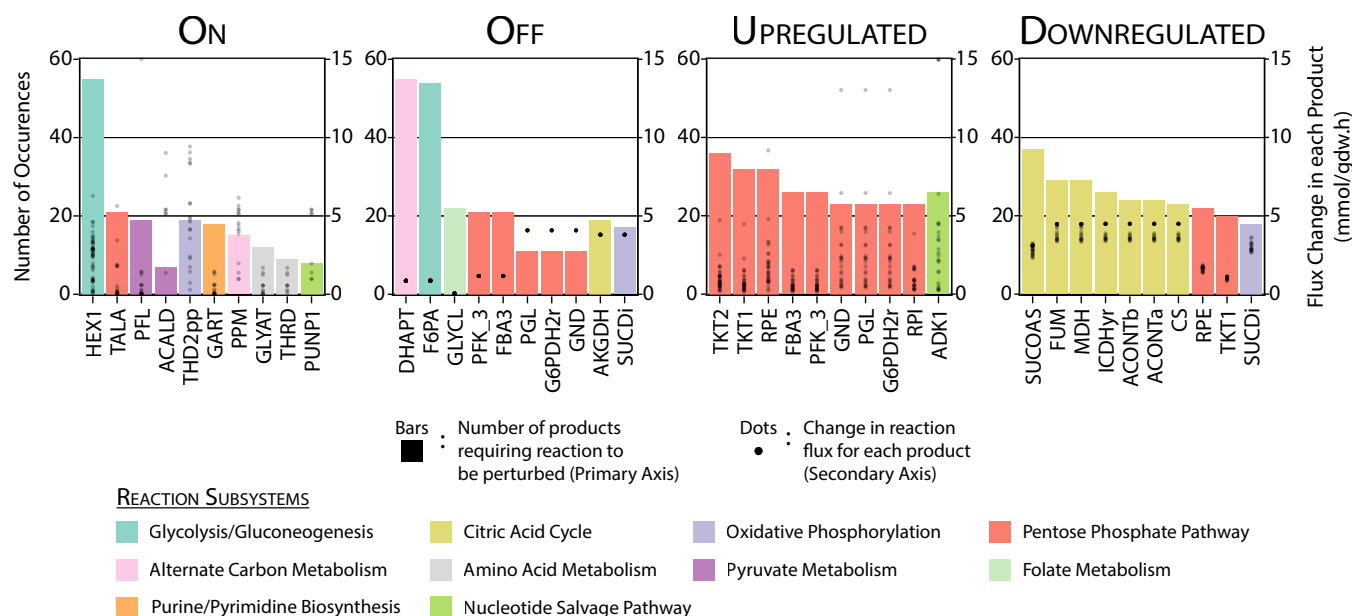


Figure 6: Most frequently occurring reactions in perturbations for TS processes in *E. coli*. Top ten frequently occurring reactions in the two-stage production strategies for native exchange metabolites in *E. coli* for *Objective I* - maximizing productivity, were obtained and classified based on the type of perturbation. The corresponding change in fluxes required in the reactions for each product are represented as dots with values in the secondary axis.

362 Among the reactions that are switched on for TS strategies (Figure 6), HEX1 (ATP dependent hexo-
 363 kinase) occurs in more than 75% of the products. This reaction serves as an alternative to the phos-
 364 phottransferase system that is used by wild-type *E. coli* to transport and phosphorylate glucose. It differs
 365 from the conventional phosphotransferase system, in that it uses ATP for phosphorylation as opposed to
 366 phosphoenolpyruvate (PEP). PEP is a key precursor to many products and therefore, alternative means
 367 of glucose usage that use less PEP are enriched in the ‘on’ type perturbations. Interestingly, the HEX1
 368 glucose transport system has previously been studied for its importance in creating platform strains for
 369 microbial chemical production⁵⁰. Furthermore, extra usage of ATP has been explored as a means to in-
 370 crease substrate uptake rates, potentially increasing product flux under low growth conditions⁵¹, suggesting
 371 the importance of studying alternatives to the native phosphotransferase system. The reaction THD2pp
 372 (NADP transhydrogenase) is also required to be switched on for many products. This likely serves to
 373 increase NADPH availability to cater to production pathways.

374 Among other types of perturbations, DHAPT (Dihydroxyacetone phosphotransferase) and F6PA (Fruc-
 375 tose 6-phosphate aldolase) are reactions that need to be turned off for most products. These also likely serve
 376 to collectively increase PEP availability for production reactions since DHAPT utilizes PEP. Many upreg-
 377 ulated reactions for *Objective I* are from the pentose phosphate pathway subsystem, serving to increase
 378 the availability of NADPH and pentose sugars for products. Surprisingly, apart from the transketolase
 379 (TKT2), none of the other reactions in the pentose phosphate pathway seem to be significantly upreg-
 380 ulated for the other two objectives. However, the overall number of upregulations is also lower in these

381 cases. TCA Cycle (Citric acid cycle) reactions are most frequently downregulated for all three objectives.

382 Notably, with the exception of the pentose phosphate pathway reactions in *Objective II* and *Objective*
383 *III*, the same reactions occur as frequent perturbations for all three objectives. Also, in the case of
384 reactions that are switched off/downregulated, some are sequential reactions({G6PDH2r, PGL, GND},
385 {FUM, MDH}, etc) and need not all be downregulated/switched off to control flux through that pathway.
386 Moreover, most of these reactions require very similar changes in their fluxes (shown as dots in Figure 6
387 and Supplementary Figure S14) for the products in which they occur. These features lend credence to
388 the possibility of the universal production strain discussed in the previous section strain and make its
389 construction more feasible.

390 4 Conclusions

391 We have seen that the choice of process type influences the process metrics and therefore the profitabil-
392 ity of a microbial chemical production process to a great extent. Furthermore, strain design choices
393 are also influenced by process choice. One-stage processes require static genetic intervention strategies
394 that couple growth and production whereas, two-stage processes require dynamic intervention strategies
395 where gene expression is temporally controlled. Recent advances in CRISPR⁵², transcriptional switches⁵³,
396 riboswitches⁵⁴, and other gene regulatory elements present an exciting outlook for the experimental im-
397 plementation of such intervention strategies. There has also been interest in computational algorithms
398 that predict dynamic control strategies which begin with high growth and switch over to growth-coupled
399 production as required by the best TS production strategies predicted in this study⁵⁵.

400 Strain engineering efforts necessary to achieve target production phenotypes predicted by mcPECASO
401 may seem daunting due to the number of perturbations required. However, it is important to note that this
402 analysis does not take into account the fact that many pathways are linear and sequential. Therefore, it
403 would not be necessary to actively perturb all fluxes predicted in this study. A reduction of the metabolic
404 network would help to identify key control reactions that actually need to be perturbed. Furthermore,
405 algorithmic approaches can be used to predict the minimal set of genetic perturbations required to achieve
406 target phenotypes given the constraints predicted by mcPECASO⁵⁶. Nevertheless, even with a large list
407 of candidate genes, it is possible to use a combination of high-throughput experiments, cell sorting and
408 a rational subset of candidates to identify which perturbations that actually lead to an improvement in
409 production characteristics, as seen in a recent study⁵⁷.

410 It is interesting to note that the production of most products involves enhancing PEP conserving and
411 NADPH overproducing strategies. The emergence of PEP as a key precursor indicates its importance as
412 a bow-tie metabolite, funneling flux into different pathways^{2,58}. Furthermore, reactions in the pentose
413 phosphate pathway seem to work in unison to increase precursor availability for number of products by
414 being upregulated or downregulated, alluding to their importance in making metabolic networks malleable
415 and robust to perturbations. These common features in strains with enhanced production of a wide
416 range of metabolites give rise to the idea of a universal production strain that could be used to maximize
417 productivity in a TS process by redirecting flux from growth to production related processes for various
418 classes of products. Such a platform strain that maximizes productivity could be realized by placing a
419 minimal number of control reactions under dynamically repressible/inducible promoters to throttle biomass
420 production flux. Tools that allow the dynamic perturbation of a large number of genes simultaneously could

421 hold the key to realizing such strains⁵². This is similar to the concept of a modular cellular chassis for the
422 production of many different compounds, that has gained interest recently^{59,60}.

423 Previous studies have only analyzed TS processes for their importance in improving process productiv-
424 ity. Here, we have shown that TS processes are able improve both process productivity and overall yield
425 for native exchange metabolites in *E. coli* even if the substrate uptake limitation caused by reduced growth
426 is considered. Since the production characteristics can be expected to be similar for other organisms and
427 non-native products too, this conclusion can be extended to products in other hosts as well. We found
428 that this conclusion holds true over a wide range of industrially relevant fermentation start parameters.
429 In future, better substrate uptake rate measurements for strains with production phenotypes will help in
430 making more accurate predictions of process performance. While it is true that the process metrics depend
431 on the substrate uptake rate of the mutant strain, we have shown that a TS process can outperform an OS
432 process, irrespective of substrate uptake characteristics for all economically relevant bioprocess objectives.
433 Further improvements in substrate uptake rates through various strategies⁶¹ will improve process metrics
434 even further. The software framework presented here - mcPECASO, has the ability to determine the effec-
435 tiveness of each process type and predict optimal hypothetical phenotypes for experimental evaluation. It
436 also provides information about the fermentation conditions under which each process type would perform
437 better. We anticipate that mcPECASO and the findings obtained in this study will be very valuable to
438 make process and strain design decisions for industrial scale production of chemicals using microorgan-
439 isms. Furthermore, the concept of a universal production strain that has the same growth phenotype and
440 several common flux perturbations identified here to switch to a production phenotype for a diverse range
441 of chemicals in a flexible manner may provide a paradigm shift in the way chemical production processes
442 are designed in the future.

443 **Acknowledgements**

444 The authors thank Ruhi Choudhary (University of Toronto) for suggesting structural edits to the manuscript
445 and Kevin Correia (University of Toronto) for insightful discussions regarding the optimization framework
446 of mcPECASO.

447 **Author's contributions**

448 KR helped formulate the study, contributed to the codebase, implemented the framework, and wrote the
449 article. NV helped formulate the study, contributed to the codebase, and edited the manuscript. RM
450 helped formulate the study, supervised the work, and edited the manuscript.

451 **Funding**

452 This work was financially supported by grants from Genome Canada, The Ontario Ministry for Research,
453 Innovation, and Science, and the National Sciences and Engineering Research Council of Canada. KR would
454 like to acknowledge funding from an Ontario Trillium Scholarship and a Mitacs Globalink Fellowship.

455 Competing interests

456 The authors declare that they have no competing interests.

457 References

- 458 [1] E. Ravasz, A. L. Somera, D. A. Mongru, Z. N. Oltvai, and A. L. Barabási. Hierarchical organization
459 of modularity in metabolic networks. *Science (80-.)*, 297(5586):1551–1555, 2002.
- 460 [2] Tamar Friedlander, Avraham E. Mayo, Tsvi Tlusty, and Uri Alon. Evolution of Bow-Tie Architectures
461 in Biology. *PLoS Comput. Biol.*, 11(3):e1004055, 2015.
- 462 [3] Kayla Nemr, Jonas E N Müller, Jeong Chan Joo, Pratish Gawand, Ruhi Choudhary, Burton Men-
463 donca, Shuyi Lu, Xiuyan Yu, Alexander F Yakunin, and Radhakrishnan Mahadevan. Engineering
464 a short, aldolase-based pathway for (R)-1,3-butanediol production in *Escherichia coli*. *Metab. Eng.*,
465 48:13–24, 2018.
- 466 [4] Kaushik Raj, Siavash Partow, Kevin Correia, Anna N Khusnutdinova, Alexander F Yakunin, and
467 Radhakrishnan Mahadevan. Biocatalytic production of adipic acid from glucose using engineered
468 *Saccharomyces cerevisiae*. *Metab. Eng. Commun.*, 6:28–32, 2018.
- 469 [5] Stephanie Galanie, Kate Thodey, Isis J. Trenchard, Maria Filsinger Interrante, and Christina D.
470 Smolke. Complete biosynthesis of opioids in yeast. *Science (80-.)*, 349(6252):1095–1100, 2015.
- 471 [6] Yanran Li, Sijin Li, Kate Thodey, Isis Trenchard, Aaron Cravens, and Christina D. Smolke. Com-
472 plete biosynthesis of noscapine and halogenated alkaloids in yeast. *Proc. Natl. Acad. Sci. U. S. A.*,
473 115(17):E3922–E3931, 2018.
- 474 [7] Weerawat Runguphan and Jay D. Keasling. Metabolic engineering of *Saccharomyces cerevisiae* for
475 production of fatty acid-derived biofuels and chemicals. *Metab. Eng.*, 21:103–113, 2014.
- 476 [8] Andreas Schirmer, Mathew A. Rude, Xuezhi Li, Emanuela Popova, and Stephen B. Del Cardayre.
477 Microbial biosynthesis of alkanes. *Science (80-.)*, 329(5991):559–562, 2010.
- 478 [9] Sang Yup Lee, Hyun Uk Kim, Tong Un Chae, Jae Sung Cho, Je Woong Kim, Jae Ho Shin, Dong In
479 Kim, Yoo Sung Ko, Woo Dae Jang, and Yu Sin Jang. A comprehensive metabolic map for production
480 of bio-based chemicals. *Nat. Catal.*, 2(1):18–33, 2019.
- 481 [10] Anthony Burgard, Mark J. Burk, Robin Osterhout, Stephen Van Dien, and Harry Yim. Development
482 of a commercial scale process for production of 1,4-butanediol from sugar. *Curr. Opin. Biotechnol.*,
483 42:118–125, 2016.
- 484 [11] C. J. Paddon, P. J. Westfall, D. J. Pitera, K. Benjamin, K. Fisher, D. McPhee, M. D. Leavell,
485 A. Tai, A. Main, D. Eng, D. R. Polichuk, K. H. Teoh, D. W. Reed, T. Treynor, J. Lenihan, H. Jiang,
486 M. Fleck, S. Bajad, G. Dang, D. Dengrove, D. Diola, G. Dorin, K. W. Ellens, S. Fickes, J. Galazzo,
487 S. P. Gaucher, T. Geistlinger, R. Henry, M. Hepp, T. Horning, T. Iqbal, L. Kizer, B. Lieu, D. Melis,
488 N. Moss, R. Regentin, S. Secrest, H. Tsuruta, R. Vazquez, L. F. Westblade, L. Xu, M. Yu, Y. Zhang,

- 489 L. Zhao, J. Lievense, P. S. Covello, J. D. Keasling, K. K. Reiling, N. S. Renninger, and J. D. Newman.
490 High-level semi-synthetic production of the potent antimalarial artemisinin. *Nature*, 496(7446):528–
491 532, 2013.
- 492 [12] David Julleson, Florian David, Brian Pfeleger, and Jens Nielsen. Impact of synthetic biology and
493 metabolic engineering on industrial production of fine chemicals. *Biotechnol. Adv.*, 33(7):1395–1402,
494 2015.
- 495 [13] Nelson R. Barton, Anthony P. Burgard, Mark J. Burk, Jason S. Crater, Robin E. Osterhout, Priti
496 Pharkya, Brian A. Steer, Jun Sun, John D. Trawick, Stephen J. Van Dien, Tae Hoon Yang, and Harry
497 Yim. An integrated biotechnology platform for developing sustainable chemical processes. *J. Ind.
498 Microbiol. Biotechnol.*, 42(3):349–360, 2015.
- 499 [14] Sang Yup Lee and Hyun Uk Kim. Systems strategies for developing industrial microbial strains. *Nat.
500 Biotechnol.*, 33(10):1061–1072, 2015.
- 501 [15] Stephen Van Dien. From the first drop to the first truckload: commercialization of microbial processes
502 for renewable chemicals. *Curr. Opin. Biotechnol.*, 24(6):1061–1068, 2013.
- 503 [16] Jens Nielsen and Jay D. Keasling. Engineering Cellular Metabolism. *Cell*, 164(6):1185–1197, 2016.
- 504 [17] Jeremy S. Edwards, Rafael U. Ibarra, and Bernhard O. Palsson. In silico predictions of Escherichia
505 coli metabolic capabilities are consistent with experimental data. *Nat. Biotechnol.*, 19(2):125–130,
506 2001.
- 507 [18] Steffen Klamt, Stefan Müller, Georg Regensburger, and Jürgen Zanghellini. A mathematical frame-
508 work for yield (vs. rate) optimization in constraint-based modeling and applications in metabolic
509 engineering. *Metab. Eng.*, 47:153–169, may 2018.
- 510 [19] Steffen Klamt and Radhakrishnan Mahadevan. On the feasibility of growth-coupled product synthesis
511 in microbial strains. *Metab. Eng.*, 30:166–178, 2015.
- 512 [20] Naveen Venayak, Kaushik Raj, Rohil Jaydeep, and Radhakrishnan Mahadevan. An Optimized
513 Bistable Metabolic Switch to Decouple Phenotypic States during Anaerobic Fermentation. *ACS Synth.
514 Biol.*, 7(12):2854–2866, 2018.
- 515 [21] Apoorv Gupta, Irene M. Brockman Reizman, Christopher R. Reisch, and Kristala L.J. Prather. Dy-
516 namic regulation of metabolic flux in engineered bacteria using a pathway-independent quorum-sensing
517 circuit. *Nat. Biotechnol.*, 35(3):273–279, 2017.
- 518 [22] Peng Xu, Lingyun Li, Fuming Zhang, Gregory Stephanopoulos, and Mattheos Koffas. Improving fatty
519 acids production by engineering dynamic pathway regulation and metabolic control. *Proc. Natl. Acad.
520 Sci. U. S. A.*, 111(31):11299–11304, 2014.
- 521 [23] Nikolaos Anesiadis, William R. Cluett, and Radhakrishnan Mahadevan. Dynamic metabolic engineer-
522 ing for increasing bioprocess productivity. *Metab. Eng.*, 10(5):255–266, 2008.

- 523 [24] Naveen Venayak, Nikolaos Anesiadis, William R. Cluett, and Radhakrishnan Mahadevan. Engineering
524 metabolism through dynamic control. *Curr. Opin. Biotechnol.*, 34:142–152, 2015.
- 525 [25] Victor Chubukov and Uwe Sauer. Environmental dependence of stationary-phase metabolism in
526 bacillus subtilis and escherichia coli. *Appl. Environ. Microbiol.*, 80(9):2901–2909, 2014.
- 527 [26] Markus W. Covert, Eric M. Knight, Jennifer L. Reed, Markus J. Herrgard, and Bernhard O. Palsson.
528 Integrating high-throughput and computational data elucidates bacterial networks. *Nature*,
529 429(6987):92–96, 2004.
- 530 [27] Eliane Fischer, Nicola Zamboni, and Uwe Sauer. High-throughput metabolic flux analysis based on
531 gas chromatography-mass spectrometry derived ¹³C constraints. *Anal. Biochem.*, 325(2):308–316,
532 2004.
- 533 [28] Uwe Sauer, Fabrizio Canonaco, Sylvia Heri, Annik Perrenoud, and Eliane Fischer. The Soluble
534 and Membrane-bound Transhydrogenases UdhA and PntAB Have Divergent Functions in NADPH
535 Metabolism of *Escherichia coli*. *J. Biol. Chem.*, 279(8):6613–6619, 2004.
- 536 [29] Annik Perrenoud and Uwe Sauer. Impact of Global Transcriptional Regulation by ArcA, ArcB, Cra,
537 Crp, Cya, Fnr, and Mlc on Glucose Catabolism in *Escherichia coli*. *J. Bacteriol.*, 187(9):3171–3179,
538 2005.
- 539 [30] Stephen S Fong, Annik Nanchen, Bernhard O Palsson, and Uwe Sauer. Latent pathway activation
540 and increased pathway capacity enable *Escherichia coli* adaptation to loss of key metabolic enzymes.
541 *J. Biol. Chem.*, 281(12):8024–8033, 2006.
- 542 [31] Bart R B van Rijsewijk, Annik Nanchen, Sophie Nallet, Roelco J Kleijn, and Uwe Sauer. Large-scale
543 ¹³C-flux analysis reveals distinct transcriptional control of respiratory and fermentative metabolism
544 in *Escherichia coli*. *Mol. Syst. Biol.*, 7(1):477, 2011.
- 545 [32] Steffen Klamt, Radhakrishnan Mahadevan, and Oliver Hädicke. When Do Two-Stage Processes Out-
546 perform One-Stage Processes? *Biotechnol. J.*, 13(2):1700539, 2018.
- 547 [33] Kai Zhuang, Laurence Yang, William R. Cluett, and Radhakrishnan Mahadevan. Dynamic strain
548 scanning optimization: An efficient strain design strategy for balanced yield, titer, and productivity.
549 DySScO strategy for strain design. *BMC Biotechnol.*, 13(1):8, 2013.
- 550 [34] Annik Nanchen, Alexander Schicker, and Uwe Sauer. Nonlinear Dependency of Intracellular Fluxes
551 on Growth Rate in Miniaturized Continuous Cultures of *Escherichia coli*. *Appl. Environ. Microbiol.*,
552 72(2):1164–1172, 2006.
- 553 [35] Nobuyoshi Ishii, Kenji Nakahigashi, Tomoya Baba, Martin Robert, Tomoyoshi Soga, Akio Kanai,
554 Takashi Hirasawa, Miki Naba, Kenta Hirai, Aminul Hoque, Pei Yee Ho, Yuji Kakazu, Kaori Sugawara,
555 Saori Igarashi, Satoshi Harada, Takeshi Masuda, Naoyuki Sugiyama, Takashi Togashi, Miki Hasegawa,
556 Yuki Takai, Katsuyuki Yugi, Kazuharu Arakawa, Nayuta Iwata, Yoshihiro Toya, Yoichi Nakayama,
557 Takaaki Nishioka, Kazuyuki Shimizu, Hirotada Mori, and Masaru Tomita. Multiple high-throughput
558 analyses monitor the response of *E. coli* to perturbations. *Science (80-.)*, 316(5824):593–597, 2007.

- 559 [36] Anke Kayser, Jan Weber, Volker Hecht, and Ursula Rinas. Metabolic flux analysis of *Escherichia coli*
560 in glucose-limited continuous culture. I. Growth-rate-dependent metabolic efficiency at steady state.
561 *Microbiology*, 151(3):693–706, 2005.
- 562 [37] Annik Nanchen, Alexander Schicker, Olga Revelles, and Uwe Sauer. Cyclic AMP-Dependent Catabo-
563 lite Repression Is the Dominant Control Mechanism of Metabolic Fluxes under Glucose Limitation in
564 *Escherichia coli*. *J. Bacteriol.*, 190(7):2323–2330, 2008.
- 565 [38] Anat Bren, Junyoung O. Park, Benjamin D. Towbin, Erez Dekel, Joshua D. Rabinowitz, and Uri
566 Alon. Glucose becomes one of the worst carbon sources for E.coli on poor nitrogen sources due to
567 suboptimal levels of cAMP. *Sci. Rep.*, 6(1):1–10, 2016.
- 568 [39] Victor Chubukov, John James Desmarais, George Wang, Leanne Jade G. Chan, Edward E.K. Baidoo,
569 Christopher J. Petzold, Jay D. Keasling, and Aindrila Mukhopadhyay. Engineering glucose metabolism
570 of escherichia coli under nitrogen starvation. *npj Syst. Biol. Appl.*, 3(1):1–7, 2017.
- 571 [40] Vincenzo Venditti, Rodolfo Ghirlando, and G. Marius Clore. Structural basis for enzyme i inhibition
572 by α -ketoglutarate. *ACS Chem. Biol.*, 8(6):1232–1240, 2013.
- 573 [41] Christopher D. Doucette, David J. Schwab, Ned S. Wingreen, and Joshua D. Rabinowitz. α -
574 ketoglutarate Coordinates Carbon and Nitrogen Utilization Via Enzyme I Inhibition. *Nat. Chem.*
575 *Biol.*, 7(12):894–901, 2011.
- 576 [42] Radhakrishnan Mahadevan, Jeremy S Edwards, and Francis J Doyle. Dynamic Flux Balance Analysis
577 of Diauxic Growth in *Escherichia coli*. *Biophys. J.*, 83(3):1331–1340, 2002.
- 578 [43] Ali Ebrahim, Joshua A. Lerman, Bernhard O. Palsson, and Daniel R. Hyduke. COBRAPy:
579 COstraints-Based Reconstruction and Analysis for Python. *BMC Syst. Biol.*, 7(1):74, 2013.
- 580 [44] Kaushik Raj, Naveen Venayak, and Radhakrishnan Mahadevan. mcpecaaso github repository. Available
581 from: <https://github.com/lmse/mcpecaaso>. Accessed 7 Apr 2020, 2020.
- 582 [45] Joao G.R. Cardoso, Kristian Jensen, Christian Lieven, Anne Sofie Lærke Hansen, Svetlana Galkina,
583 Moritz Beber, Emre Özdemir, Markus J. Herrgård, Henning Redestig, and Nikolaus Sonnenschein.
584 Cameo: A Python Library for Computer Aided Metabolic Engineering and Optimization of Cell
585 Factories. *ACS Synth. Biol.*, 7(4):1163–1166, 2018.
- 586 [46] Jeffrey D Orth, Tom M Conrad, Jessica Na, Joshua a Lerman, Hojung Nam, Adam M Feist, and
587 Bernhard Ø Palsson. A comprehensive genome-scale reconstruction of *Escherichia coli* metabolism–
588 2011. *Mol. Syst. Biol.*, 7(535):535, 2011.
- 589 [47] Nathan E. Lewis, Kim K. Hixson, Tom M. Conrad, Joshua A. Lerman, Pep Charusanti, Ashoka D.
590 Polpitiya, Joshua N. Adkins, Gunnar Schramm, Samuel O. Purvine, Daniel Lopez-Ferrer, Karl K.
591 Weitz, Roland Eils, Rainer König, Richard D. Smith, and Bernhard Palsson. Omic data from evolved
592 E. coli are consistent with computed optimal growth from genome-scale models. *Mol. Syst. Biol.*,
593 6(390):390, 2010.

- 594 [48] R Mahadevan and C H Schilling. The effects of alternate optimal solutions in constraint-based genome-
595 scale metabolic models. *Metab. Eng.*, 5(4):264–276, 2003.
- 596 [49] Kaushik Raj, Naveen Venayak, and Radhakrishnan Mahadevan. Novel two-stage processes for optimal
597 chemical production in microbes - github repository. Available from: [https://github.com/lmse/
598 novel_two_stage](https://github.com/lmse/novel_two_stage). Accessed 7 Apr 2020, 2020.
- 599 [50] Verónica Hernández-Montalvo, Alfredo Martínez, Georgina Hernández-Chavez, Francisco Bolivar, Fer-
600 nando Valle, and Guillermo Gosset. Expression of galP and glk in a *Escherichia coli* PTS mutant
601 restores glucose transport and increases glycolytic flux to fermentation products. *Biotechnol. Bioeng.*,
602 83(6):687–694, 2003.
- 603 [51] Simon Boecker, Ahmed Zahoor, Thorben Schramm, Hannes Link, and Steffen Klamt. Broadening the
604 Scope of Enforced ATP Wasting as a Tool for Metabolic Engineering in *Escherichia coli*. *Biotechnol.*
605 *J.*, 14(9):1800438, 2019.
- 606 [52] Alexander C. Reis, Sean M. Halper, Grace E. Vezeau, Daniel P. Cetnar, Ayaan Hossain, Phillip R.
607 Clauer, and Howard M. Salis. Simultaneous repression of multiple bacterial genes using nonrepetitive
608 extra-long sgRNA arrays. *Nat. Biotechnol.*, 37(11):1294–1301, 2019.
- 609 [53] Jeong Wook Lee, Andras Gyorgy, D. Ewen Cameron, Nora Pyenson, Kyeong Rok Choi, Jeffrey C.
610 Way, Pamela A. Silver, Domitilla Del Vecchio, and James J. Collins. Creating Single-Copy Genetic
611 Circuits. *Mol. Cell*, 63(2):329–336, 2016.
- 612 [54] Abigail N. Leistra, Nicholas C. Curtis, and Lydia M. Contreras. Regulatory non-coding sRNAs in
613 bacterial metabolic pathway engineering. *Metab. Eng.*, 52:190–214, 2019.
- 614 [55] Naveen Venayak, Axel von Kamp, Steffen Klamt, and Radhakrishnan Mahadevan. MoVE identifies
615 metabolic valves to switch between phenotypic states. *Nat. Commun.*, 9(1):5332, 2018.
- 616 [56] Radhakrishnan Mahadevan, Axel Von Kamp, and Steffen Klamt. Genome-scale strain designs based
617 on regulatory minimal cut sets. *Bioinformatics*, 31(17):2844–2851, 2015.
- 618 [57] Raphael Ferreira, Christos Skrekas, Alex Hedin, Benjamín J. Sánchez, Verena Siewers, Jens Nielsen,
619 and Florian David. Model-Assisted Fine-Tuning of Central Carbon Metabolism in Yeast through
620 dCas9-Based Regulation. *ACS Synth. Biol.*, 8(11):2457–2463, 2019.
- 621 [58] Jing Zhao, Hong Yu, Jian Hua Luo, Zhi Wei Cao, and Yi Xue Li. Hierarchical modularity of nested
622 bow-ties in metabolic networks. *BMC Bioinformatics*, 7(1):386, 2006.
- 623 [59] Sergio Garcia and Cong T. Trinh. Multiobjective strain design: A framework for modular cell engi-
624 neering. *Metab. Eng.*, 51:110–120, 2019.
- 625 [60] Brandon Wilbanks, Donovan S. Layton, Sergio Garcia, and Cong T. Trinh. A Prototype for Modular
626 Cell Engineering. *ACS Synth. Biol.*, 7(1):187–199, 2018.
- 627 [61] Qiang Yan and Stephen S. Fong. Increasing carbon source uptake rates to improve chemical produc-
628 tivity in metabolic engineering. *Curr. Opin. Biotechnol.*, 53:254–263, 2018.